Electroless Ni-P-Al_2O_3 composite coatings on Al-Si casting alloy

D. Vojtěch*, F. Blanc, P. Novák, T. Fabián

Department of Metals and Corrosion Engineering, Institute of Chemical Technology, Prague, Technická 5, 166 28 Prague 6, Czech Republic

Received 16 July 2007, received in revised form 17 December 2007, accepted 22 February 2008

Abstract

Composite Ni-P-Al_2O_3 coatings were prepared on pre-treated Al and Al-Si casting alloy by electroless deposition in suspensions of 5–20 g l^{-1} Al_2O_3 in a solution containing nickel lactate, nickel hypophosphite and lactic acid. In the as-deposited coatings, ceramic particles were homogeneously distributed in extremely fine-grained nanocrystalline Ni-P matrix. Adhesion of coatings to substrate was better in case of Al-Si alloy due to silicon present in its structure. Hardness, P content and grain size of the Ni-P matrix were 549–574 HV, 10.0 wt.% and 1.9 nm, respectively. These attributes did not depend either on Al_2O_3 volume fraction or on substrate chemical composition. The relatively low hardness value was discussed with respect to the inverse Hall-Petch effect. Due to composite coatings, abrasion resistance of Al-based alloys was significantly increased. The strongest effect was observed after deposition in a bath containing 5 g l^{-1} Al_2O_3. Further additions of ceramic particles to the bath did not have so strong effect on abrasion resistance. Heat treatment of composite coatings at 400 °C/1 h induced decomposition of Ni-P phase to Ni and Ni_3P that led to significant hardening (almost 1000 HV) of the Ni-P matrix. The coatings were also heat treated at 500 °C/24 h that simulated solution annealing. This heat treatment led to an excessive softening of Ni-P matrix. In addition, solid state reaction between Al and Ni produced layers of hard Al_3Ni_2 and Al_3Ni intermetallics.

K e y w o r d s: Al-Si alloy, aluminium, Ni-P-Al_2O_3 coating, heat treatment, abrasion, hardness

1. Introduction

Importance of aluminium-based alloys in automotive industry shows growing tendency due to their low weight and high specific strength. Casting alloys based on the Al-Si system have excellent casting properties and are thus suitable for production of large-series of complex-shape components, such as engine blocks, pistons, cylinder liners etc. In some applications (cylinder liners, pistons), however, they suffer from insufficient wear resistance. To prolong the life time of components, several approaches have been adopted in industrial scale. They involve reinforcement with particles or fibres producing Al-Si matrix composites [1], increase of Si content in alloys [2], hard coatings. The hard PVD or electrodeposited chromium coatings offer sufficient improvement of hardness and wear resistance of Al-Si alloys but problems often arise when components of complex shapes are coated. These problems are in part avoided when using electroless Ni-P coatings.

The electroless Ni-P coatings are produced by relatively simple and low cost process and provide significant improvement of wear and corrosion resistance of various materials. The process is based on a redox reaction in which Ni^{2+} ions are reduced by sodium hypophosphite (NaH_2PO_2) on a substrate surface [3]. It has been shown by many studies that the physical properties of Ni-P deposits can vary depending on internal structure and P content. Hardness of as-deposited coatings between 500 and 700 HV is generally obtained [4]. An appropriate heat treatment (e.g. 400 °C/1 h) is able to increase hardness significantly, due to crystallization of amorphous Ni-P phase and formation of hard nickel phosphides [5]. Further improvement of hardness and wear resistance can be achieved by a co-deposition of hard particles, such as boron carbide, silicon carbide, diamond, aluminium

*Corresponding author: tel.: +420 22 044 42 90; fax: +420 22 044 44 00; e-mail address: Dalibor.Vojtech@vscht.cz

Table 1. Chemical composition of coated materials (in wt.%)

Substrate	Si	Fe	Mg	Mn	Cu	Ti	Al
Al	0.04	0.06	0.05	0.10	–	–	rem.
Al-Si	11.83	0.12	0.06	0.18	0.04	0.1	rem.

oxide, etc., producing composite coatings [6, 7]. There are a lot of papers on the electroless composite coatings, but majority of them are devoted to coatings on steel substrates [8]. The important difference between steel and aluminium substrates is that aluminium easily forms the stable passive oxide layer on its surface which reduces adhesion of the coating. Hence, a chemical pre-treatment of aluminium substrate removing the oxide is necessary and, sometimes, additional Zn or Pd activation is used [9].

The presented paper is devoted to the electroless Ni-P-Al_2O_3 composite coating. Aluminium oxide is used as reinforcement because of its low cost and availability with various granulometric parameters. The main objective of this work is to demonstrate possibility to deposit this coating on the Al-Si casting alloy and to describe parameters of the coated material. The coating was deposited also on pure aluminium in order to illustrate positive influence of silicon in the substrate.

2. Experimental

Commercial pure aluminium (99.7 wt.% Al) and Al-12wt.%Si alloy, see Table 1, were used as substrates for electroless deposition. The materials were melted in an electric resistance furnace and cast into cast-iron metal mould to prepare cylindrical castings with diameter of 20 mm. Cylindrical samples with length of 10 mm were cut directly from these castings. Surface of samples was mechanically grinded by P60–P1200 SiC papers to obtain defined surface roughness of 3 μm.

Pre-treatment of the substrate surface included following steps, according to the standard procedure recommended by industrial supplier of coating baths:

– ultrasonic degreasing in acetone,
– rinsing,
– deoxidizing in 10 % HCl,
– rinsing,
– deoxidizing in 10 % H_2SO_4,
– rinsing in demineralized water.

Zincating treatment was not used in our experiment.

In order to find the most appropriate deposition conditions, a series of coating experiments was performed using Al_2O_3 particles in various Ni-P deposition baths. The applied deposition conditions were found either in literature or in industrial procedures. Various parameters were evaluated, such as deposition rate, uniformity of coating, adherence of coating to substrate and ability of bath to co-deposit aluminium oxide particles. Finally, deposition conditions specified in Table 2 were selected which provided the best properties of coatings.

Table 2. Conditions used for electroless deposition of the Ni-P-Al_2O_3 composite coatings

Parameters of deposition	
Chemical composition of the bath	nickel lactate $Ni(C_3H_5O_3)_2$ – 30 g l^{-1} nickel hypophosphite $Ni(H_2PO_2)_2$ – 20 g l^{-1} lactic acid $C_3H_6O_3$ – 10 ml l^{-1} Al_2O_3 particles – 0–20 g l^{-1}
Temperature	90 °C
pH	4.5–5.0
Bath volume	500 ml
Deposition time	120 min

Aluminium oxide (irregular particles, average particle size of 5 μm) provided by an industrial supplier was used as reinforcement in the composite coatings. Prior to deposition, a weighed amount of Al_2O_3 particles (0–20 g l^{-1}) was added to the bath and homogeneous distribution of particles was ensured by a magnetic stirrer (rod of 2 cm in length placed at the bottom of the deposition bath) rotating at a rate of 4000 rpm. The substrates for deposition were placed at the bottom of the bath. After deposition, a part of coated samples was heat treated by a regime recommended to obtain maximum hardness of the Ni-P deposits (400 °C/1 h) [5]. In addition, composite coated Al-Si alloy was also annealed at 500 °C/24 h. This regime in part simulates real thermal loading of Al-Si castings during their solution annealing.

Structure of both as-deposited and as-heat treated Ni-P-Al_2O_3 composite coatings was examined by light microscopy (LM), scanning electron microscopy (SEM-HITACHI S 4700) with energy dispersive X-ray spectrometer (EDS-Noran) and by X-ray diffraction analysis (XRD-X'PERT PRO). Hardness HV 0.005 of the Ni-P phase in coatings was measured on the cross-sections (10 measurements for each sample). Wear resistance of the coated samples at room temperature was determined by using the modified "pin-on-disc" method. In this method, the cylindrical samples were moved on the grinding SiC paper P4000, the total sliding distance was 333 m and the normal force was 5.8 N

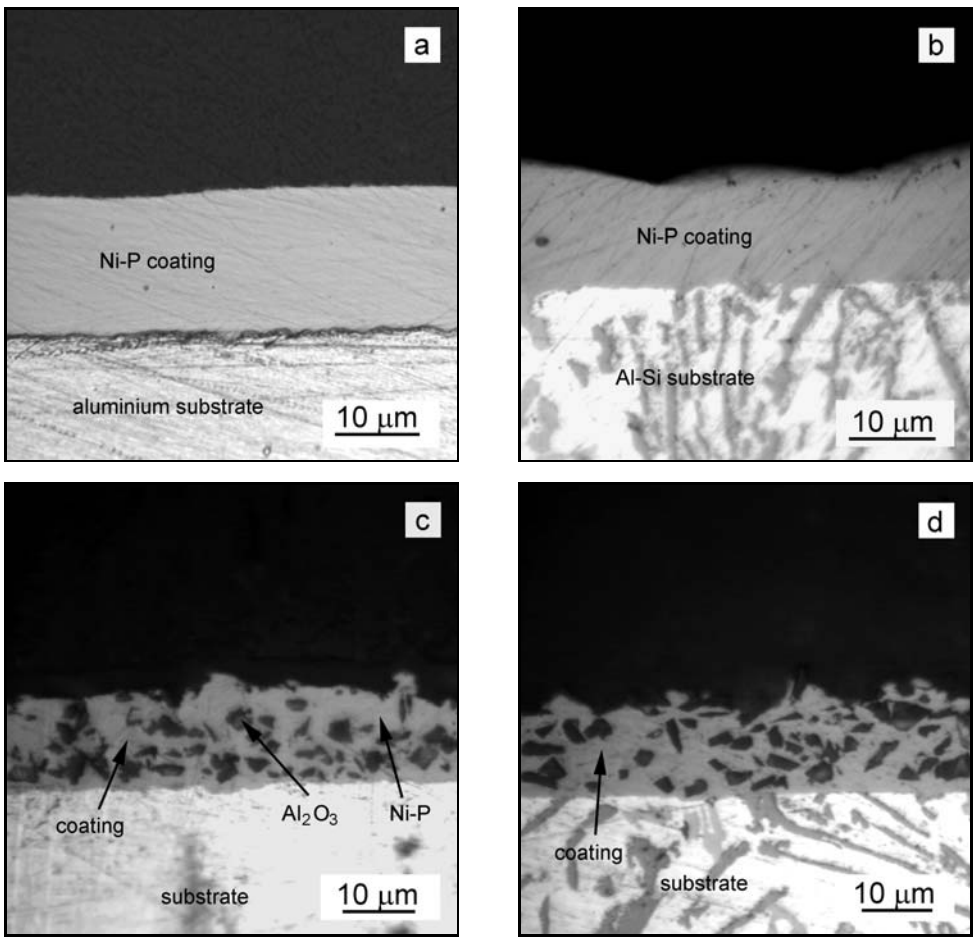

Fig. 1. Cross-sectioned Ni-P coatings (a, b) and Ni-P-Al_2O_3 composite coatings (c, d) on both Al (a, c) and Al-Si alloy (b, d). The composite coatings were deposited from a bath containing 15 g l^{-1} Al_2O_3 (light microscope).

[10]. Abrasion was expressed in term of thickness loss during the wear tests.

3. Results and discussion

3.1. Structure of as-deposited coatings

Optical micrographs of the cross-sectioned Ni-P and Ni-P-Al_2O_3 composite coatings on both Al and Al-Si alloy are illustrated in Fig. 1a–d. It can be seen that the Al_2O_3 particles (dark) are uniformly distributed in the coatings. The thickness of composite coatings varies between 15 and 22 μm that gives an average deposition rate of about 8–11 μm h^{-1} which is similar or slightly lower than those reported elsewhere [7]. It is also observed that the thickness is not modified significantly by substrate composition. Detailed observation of large surface areas of coated samples indicates that aluminium and Al-Si alloy differ in terms of coating adherence and homogeneity. This is illustrated in Fig. 2a,b that shows overall views on the cross-sectioned coatings. The composite coating on the Al-Si alloy seems to exhibit a good adherence to the substrate, since no voids are observed between coating and substrate. In addition, this coating has uniform thickness and particle distribution. In contrast, the adherence of coating on the pure aluminium seems to be worse, see also Figs. 1a,b. A number of places where the coating is avoided, probably due to metallographic sample preparation, can be observed. The coating thickness is not uniform, either. If we consider that both materials were treated in exactly the same way, the Al-Si casting alloy appears better substrate for the electroless Ni-P-Al_2O_3 composite coating than aluminium. A reason may lie in the existence of the oxide passive layer. This layer forms rapidly both in air and in water solutions and uniformly covers the surface. During the electroless deposition, the passive layer reduces the coating adherence to the substrate. In the case of pure Al, the passive layer may be present on the whole surface in spite that the appropriate pretreatment was used in our experiment. The Al-Si alloy, on the other hand, contains a relatively large fraction of silicon particles in the structure that are less prone

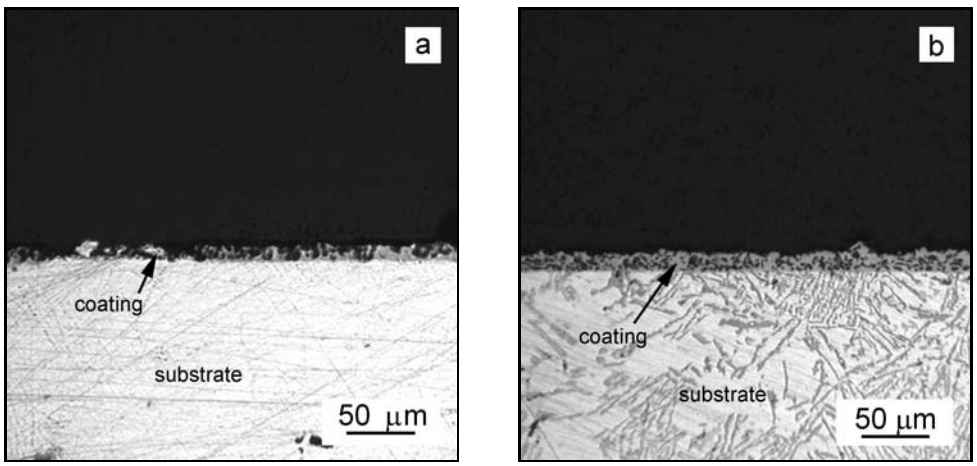

Fig. 2. Overall views on the cross-sectioned Ni-P-Al_2O_3 composite coatings on Al (a) and Al-Si (b). The coatings were deposited from a bath containing 20 g l^{-1} Al_2O_3 (light microscope).

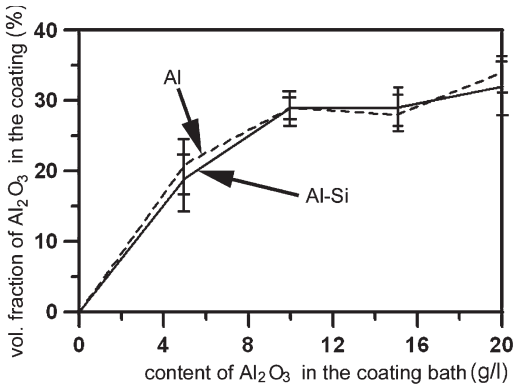

Fig. 3. Volume fraction of aluminium oxide in the coatings versus its amount in the bath.

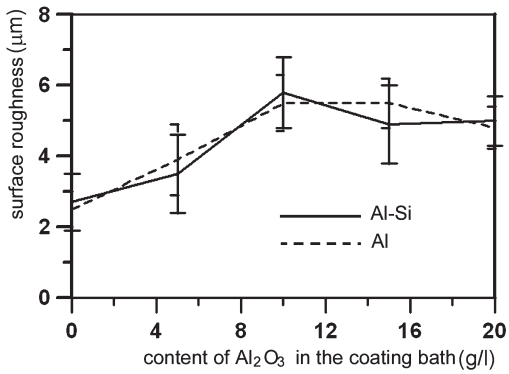

Fig. 4. Surface roughness as a function of aluminium oxide content in the bath.

to form passive layers. The problems arising from the passive layer on aluminium would be removed by, e.g., zincating pre-treatment.

Figure 3 shows plots of volume fraction of aluminium oxide in the coating versus its amount in the bath. It is evident that the content of hard particles in the coating increases, as their amount in the bath grows. Maximum volume fraction of hard particles is about 30 %. In contrast, the co-deposition of finer (1 μm, 0.3 μm, 50 nm) alumina particles in electroless Ni-P was reported to be slower [7]. After deposition from a bath containing 6 g l^{-1} of particles the coatings contained 8, 4 and 2 wt.% of 1 μm, 0.3 μm, 50 nm alumina particles, respectively. Perhaps, smaller particles are more easily swept away by moving liquid from a substrate. It can be also seen in Fig. 3 that the volume content of hard particles grows rapidly only up to 10 g l^{-1} of particles in the bath. This value corresponds to about 29 vol.% of particles in the coating. Addition of further 10 g l^{-1} of oxide particles to the bath leads only to a slight increase of their amount in the coating. Therefore, too high amount of oxide in the bath does not seem to be very useful. The reason is that in highly concentrated suspensions, the rate of particle co-deposition is not driven by particle content in the bath but rather by Ni-P deposition rate that does not seem to be affected by particles significantly. Additionally, large volume contents of hard particles in the coating would not be favourable, since such particles would be susceptible to detachment from the Ni-P matrix.

Figure 4 expresses the average surface roughness as a function of aluminium oxide content in the bath. This parameter behaves similarly like that in Fig. 3. The smoothest surface is characteristic for pure Ni-P layer, while co-depositing particles increase roughness but only up to a maximum at 10 g l^{-1} of particles. Then the roughness remains nearly constant. The fact, that the surface roughness reflects the amount of relatively coarse co-depositing particles in the bath and hence in the coatings, is consistent with other authors [7].

Concentration of phosphorus in common electroless Ni-P coatings moves around 3–14 wt.% [4]. There-

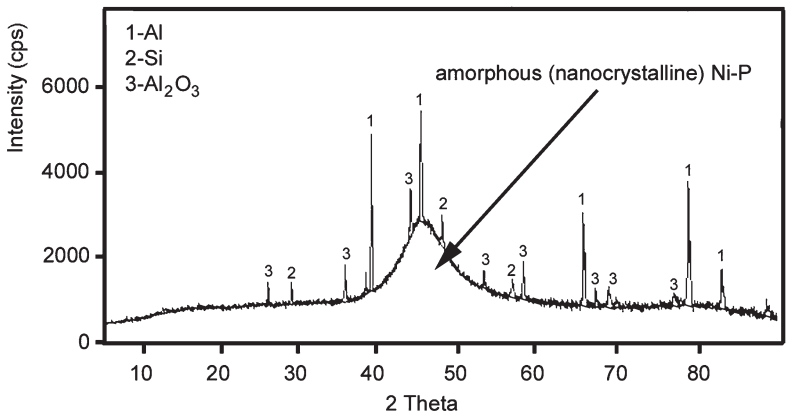

Fig. 5. XRD pattern of the as-deposited Ni-P-Al_2O_3 composite coating (a bath containing 5 g l^{-1} Al_2O_3 was used).

fore, the P-content measured by EDS in both pure Ni-P and Ni-P-Al_2O_3 composite coatings – **10.0 ± 0.8 wt.%** – appears relatively high. In spite of some scatter of obtained values, the P-concentration does not seem to depend significantly on particle volume fraction in the coating and on substrate material. High concentration of phosphorus has a basic influence on the coating hardness, as will be shown later. XRD pattern of the as-deposited composite coating is illustrated in Fig. 5. It contains a single broad amorphous peak of Ni-P and sharp well separated peaks of Al_2O_3, Al and Si. Due to a limited ability of XRD to distinguish between purely amorphous and extremely finely nanocrystalline phase, the broad peak is commonly regarded as corresponding to a nanocrystalline phase composed of extremely fine nanometer scaled crystalline regions surrounded by amorphous grain boundaries. The crystalline grain size D can be estimated from the Ni line broadening β (the peak width in the half of its height) and X-ray wavelength λ by using the Scherrer formula:

$$D = 0.9\lambda/\beta\cos\theta, \qquad (1)$$

where θ is the diffraction angle. In our case, the average grain size is estimated as **1.9 nm** that is in a good accordance with other values reported for Ni-P electroless deposits [3]. It should be noted that this parameter is not influenced either by particle volume fraction in the coating or by substrate material.

3.2. Hardness and wear resistance of as-deposited coatings

Hardness of Ni-P phase versus alumina particle content in the coating is listed in Table 3. The values lie between approx. 540 and 580 HV 0.005. In spite of some random variations, no dependence of hardness either on alumina content or on substrate is seen. Since hardness is determined mainly by P-content [4], it means that co-deposition of alumina does not influence the amount of phosphorus in the Ni-P phase, as was proved also by EDS, see above. Similar results have been reported e.g. in [6, 7], where Ni-P-Al_2O_3 and Ni-P-SiC composites were studied.

Table 3. Hardness HV 0.005 of the Ni-P matrix versus Al_2O_3 content in the Ni-P-Al_2O_3 composite coatings

	Volume content of alumina particles in the coating (vol.%)					
Substrate	0	19	21	29	32	33
Al	555	–	552	574	–	563
Al-Si	574	562	–	549	563	–

When we compare the measured hardness in Table 3 with published data [4], it appears to be relatively low. In commercial as-deposited coatings the Ni-P matrix commonly achieves hardness up to 700 HV. As was indicated before, hardness of the Ni-P phase is directly related to P-concentration. The tendency of increasing hardness with reducing amount of phosphorus has been proved by a number of authors. It was for example shown that hardness of about 650 HV corresponds to approx. 4 wt.% of P, while Ni-10 wt.% P phase achieves only about 550 HV [3] that is consistent with our results.

Reasons for the strong influence of phosphorus on hardness of Ni-P deposits still remain under discussion, but some indications have already been reported. It is believed that phosphorus modifies atomic structure of the nanocrystalline Ni-P phase. Due to a difference in atomic radii of Ni and P that are 1.25 and 1.09 Å, respectively [11], phosphorus induces internal stress in Ni lattice. As a consequence, structure transforms in such a way that nanocrystalline grains become refined, as phosphorus concentration grows. In others words, since phosphorus can be dissolved in nanocrystalline solid solution only to some extent, high P-concentration produces a large volume frac-

tion of fully amorphous grain boundaries, i.e. fraction of amorphous phase grows. This was illustrated in [3], where Ni-P deposits with 3.9 and 10.2 wt.% P were composed of nanocrystals with size of 3.0 and 1.5 nm, respectively. The effect of phosphorus on microstructure of Ni-rich phase in electroless coatings is similar to that in rapidly solidified alloys containing Ni, Fe or Co as a basic metal and C, Si, P or B as additives. These systems with unique magnetic properties have been known to readily form nanocrystalline and even amorphous phases.

It remains to answer a question – why a phase composed of finer grains is softer than that composed of coarser grains. This finding is not in accordance with the Hall-Petch relation, which well applies to industrial alloys:

$$HV = K_1 + K_2/d^{1/2}. \quad (2)$$

It has been shown in a number of papers that nanocrystalline systems with grain size d in order of tens nm and less behave according to so called inverse Hall-Petch (H-P) behaviour, i.e. the smaller the grains are present, the lower the hardness and yield strength is obtained [12–22]. It is generally agreed that the inverse H-P effect results from a high volume fraction of grain boundaries and triple junctions in nanocrystalline materials [12, 15, 16-22]. It is for example demonstrated that a material with an average grain size of 5 nm contains about 50 vol.% of grain boundaries and triple junctions [19]. The plastic deformation of such finely grained metal can not be controlled by the dislocation slip since the activation of dislocation sources in grains surrounding a dislocation pile-up would demand extremely high stress, much higher than that observed experimentally. Therefore, interfaces between grains begin to play an active role in deformation process instead of dislocations inside grains. Various theoretical models have been proposed to explain the inverse H-P effect, i.e. to explain a relatively low stress needed for grain boundary activity to start. These models include e.g. grain boundary diffusion (Coble creep) [12, 20], grain boundary sliding [14, 18] or grain boundary viscoelastic deformation [12]. However, each of these models is consistent only with limited sets of experimental data. Therefore, the exact explanation of the inverse H-P effect still seems to remain unanswered.

Results of abrasion tests are summarized in Fig. 6a, b where abrasion behaviour is expressed as thickness loss versus abrasion distance. Uncoated samples are also included in this figure for comparison. It is observed that the Ni-P coating alone reduces abrasion rate by about 50 percent for both Al and Al-Si substrate, compare curves A and B in Fig. 6a,b. Incorporation of hard ceramic particles into Ni-P coating leads to further significant improvement of abrasion resistance. By comparing of curve B and C it is seen that the

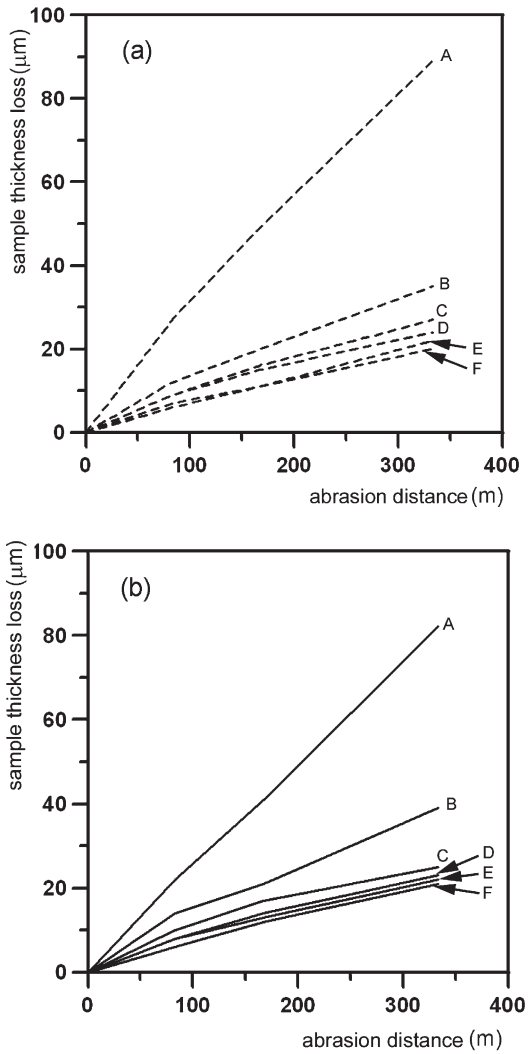

Fig. 6. Abrasion behaviour expressed as thickness loss versus abrasion distance: a) Al substrate, b) Al-Si substrate. Curves: A – uncoated substrate, B – Ni-P coating, C – Ni-P-Al_2O_3 coating (bath with 5 g l^{-1} Al_2O_3), D – Ni-P-Al_2O_3 coating (bath with 10 g l^{-1} Al_2O_3), E – Ni-P-Al_2O_3 coating (bath with 15 g l^{-1} Al_2O_3), F – Ni-P-Al_2O_3 coating (bath with 20 g l^{-1} Al_2O_3).

bath containing 5 g l^{-1} Al_2O_3 is the most effective in this sense. It is also important to note that further additions of ceramic particles to the bath do not have so strong effect on abrasion resistance. These results are consistent with volume fractions of particles in coatings shown in Fig. 3. The bath containing 5 g l^{-1} Al_2O_3 produces coatings containing about 20 vol.% of hard particles. However, higher contents of aluminium oxide in the bath do not lead to proportional increase of its volume fraction in coatings. Abrasion resistance is a complex parameter which depends primarily on the coating hardness, i.e. on the ceramic particles content. However, other coating parameters, such as roughness of coating surface, should be taken into account. It can

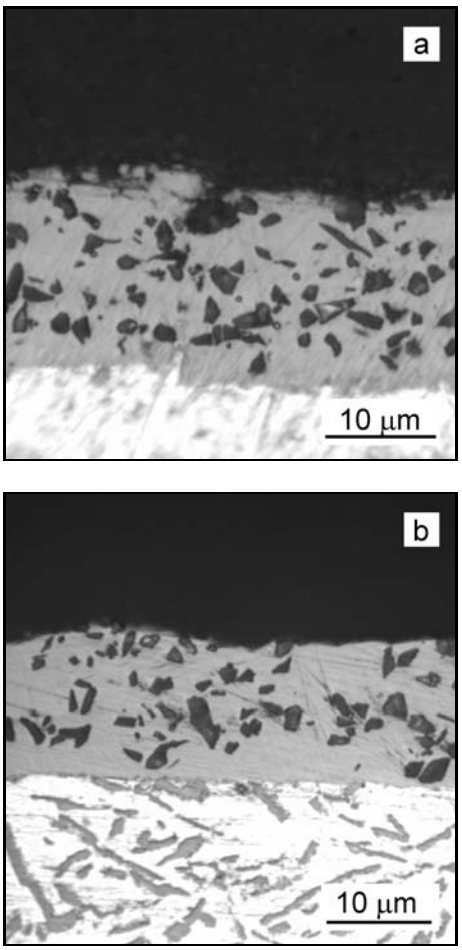

Fig. 7. Cross-section of heat treated (400 °C/1 h) composite coatings obtained by deposition in the bath containing 5 g l^{-1} Al_2O_3: a) Al substrate, b) Al-Si substrate (light microscope).

be assumed that an increase of roughness negatively affects abrasion resistance, since surface parts of such coatings are more prone to mechanical detachment. It is illustrated in Fig. 4 how surface roughness grows as content of aluminium oxide in the bath increases. Therefore, surface roughness may be another reason for small differences in abrasion rate between coatings produced in bath with 5 g l^{-1} Al_2O_3 and more (curves C – F in Fig. 6a,b).

3.3. Influence of heat treatment

The Al and Al-Si substrates with composite coatings were heat treated by a commonly recommended regime, i.e. annealing at **400 °C/1 h** [4, 5]. Cross-section of composite coatings obtained by deposition in the bath containing 5 g l^{-1} Al_2O_3 is shown in Fig. 7a,b. It is evident that the annealing does not influence appearance of coatings markedly. The hard particles (dark) still remain homogeneously distributed across the coatings. Moreover, no layer of reaction products between Ni-P coating and substrate is observed what means that the temperature is too low to induce interdiffusion of Al and Ni.

Table 4. Hardness HV and abrasion resistance (expressed as thickness loss ΔL after 333 m abrasion) of as-prepared and as-heat treated (400 °C/1 h) coatings (composite coating was prepared in the bath containing 5 g l^{-1} Al_2O_3; properties of uncoated substrates are also included for comparison; hardness of the composite coatings corresponds to Ni-P phase)

Coating	Substrate	HV*	ΔL (μm)
Uncoated	Al	25	89
	Al-Si	70	82
Ni-P as-prepared	Al	555	35
	Al-Si	574	39
Ni-P-Al_2O_3 as-prepared	Al	552	27
	Al-Si	562	25
Ni-P-Al_2O_3 as-heat treated	Al	976	18
	Al-Si	944	19

*HV 5 for uncoated substrates and HV 0.005 for Ni-P phase in the coatings

In Table 4, hardness and abrasion resistance of the heat treated coating is compared to uncoated substrate, as well as to as-deposited coating. It is observed that the applied heat treatment markedly improves hardness and abrasion resistance. After heat treatment, the Ni-P layer has hardness of almost double that of the as-prepared coating. Due to high hardness of the Ni-P matrix, abrasion rate of composite coating reduces by nearly 30 %.

Figure 8 shows XRD pattern of the composite coating prepared in the bath with 5 g l^{-1} Al_2O_3 and heat treated at 400 °C/1 h. Sharp and well separated peaks of several crystalline phases are found after heat treatment, instead of the single broad peak corresponding to extremely fine nanocrystalline nature of Ni-P phase in the as-prepared coating (Fig. 5). Beside Al, Si and Al_2O_3 that are identified also in the as-prepared coating, presence of crystalline Ni and Ni_3P phases are proved. It is known that extremely fine nanocrystalline structure with almost homogeneous distribution of phosphorus is not very thermally stable. Annealing at 400 °C is sufficient to accelerate diffusion rate of phosphorus and to induce precipitation of very fine phosphide particles [4]. Hard phosphides in plastic Ni matrix act as effective obstacles for slip of dislocations. As a result, hardness that is directly related to the yield strength increases.

In contrast to the preceding heat treatment, annealing at **500 °C/24 h** significantly modifies appearance of the composite coating, as is illustrated in

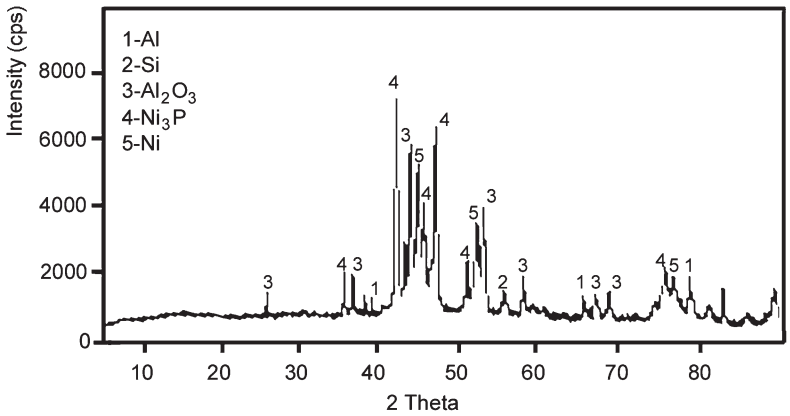

Fig. 8. XRD pattern of the heat treated (400 °C/1 h) composite coating prepared on Al-Si alloy in the bath with 5 g l^{-1} Al_2O_3.

Table 5. Chemical composition (at.%) (measured by EDS), phase composition (estimated from chemical composition) and hardness HV 0.005 of the three sublayers in Fig. 9 formed from the composite coating due to annealing at 500 °C/24 h

Sublayer	Al	Si	Ni	P	HV 0.005	Present phases
1*	1.1	0.4	86.4	12.1	335	Ni, Ni_3P
2	51.2	3.1	44.1	1.6	984	Al_3Ni_2
3	66.1	3.5	28.6	1.8	765	Al_3Ni

* all parameters refer to the Ni-P matrix

Fig. 9 for the coating prepared in the bath with 5 g l^{-1} Al_2O_3. At least three sub-layers denoted as 1–3 can now be distinguished. Their hardness, chemical and phase composition are summarized in Table 5. **Sublayer 1** is a remaining part of the original composite coating, since it contains both Ni-P matrix and ceramic particles. Due to annealing, nanocrystalline homogeneous Ni-P phase decomposes to form pure Ni and phosphide particles, similarly to the preceding heat treatment. At 500 °C, however, growth of phosphide particles and Ni grains brings about a considerable softening of the Ni-P alloy. **Sublayers 2 and 3** result from an intensive inward and outward diffusion flows of Ni and Al, respectively. They are dominated by products of solid state reaction between Al and Ni, i.e. by intermetallic phases Al_3Ni_2 (sublayer 2) and Al_3Ni (sublayer 3) with minor additions of Si and P. These intermetallics show increased hardness, especially Al_3Ni_2 phase, due to ordered structure which is unfavourable for the dislocation slip.

High hardness of intermetallics in part balances the softening of Ni-P alloy, hence the effect of applied thermal loading on hardness does not seem to be fully negative. However, adhesion of coating seems to be slightly reduced due to annealing at 500 °C, since cracks create at intermetallic/substrate interface (marked by arrows in Fig. 9). These defects may form upon cooling from annealing temperature due to differences in thermal expansion between Al and Al-Ni intermetallics. Influence of heat treatment on adhesion of composite coatings thus needs further research.

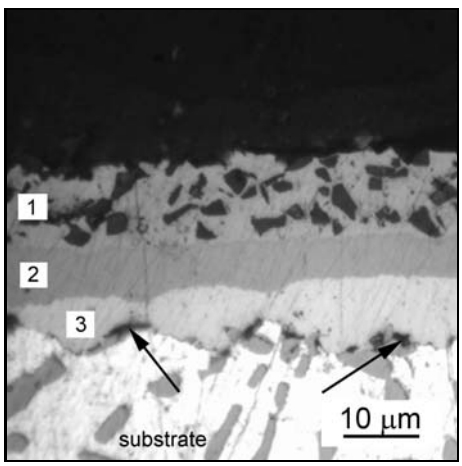

Fig. 9. Cross-section of heat treated (500 °C/24 h) composite coating on Al-Si alloy with sublayers 1–3 and with cracks at intermetallic/substrate interface (marked by arrows) (deposition was carried out in the bath containing 5 g l^{-1} Al_2O_3) (light microscope).

4. Conclusions

It is shown in the presented paper that hard

Ni-P-Al_2O_3 composite coatings can be successfully prepared on pre-treated Al-Si casting alloy by co-deposition of hard particles from stirred bath containing nickel lactate, nickel hypophosphite and lactic acid. Aluminium oxide content in the bath of about $10\,g\,l^{-1}$ ensures a sufficient volume fraction of particles in the deposit. Due to silicon particles in the structure of Al-Si substrate, adhesion of composite coatings is better than that on pure Al. Composite coatings can be used to significantly improve abrasion resistance of Al-Si castings, especially if they are subsequently heat treated at 400 ℃/1 h. When castings are heat treated at higher temperatures, e.g. solution annealed at 500 ℃ and more, hard intermetallic reaction products form and coating adhesion may reduce due to cooling or heating.

Acknowledgements

The research on electroless composite coatings is financially supported by the research projects no. MSM6046137 302 and 104/08/1102.

References

[1] KAINER, K. U.: Metal Matrix Composites. Weinheim, WILEY-VCH 2006.
[2] DAVIS, J. R.: Aluminium and Aluminium Alloys. Materials Park OH, ASM International 1993.
[3] APACHITEI, I.—DUSZCZYK, J.: Surf. Coat. Technol., *132*, 2000, p. 89.
[4] KEONG, K. G.—SHA, W.—MALINOV, S.: Surf. Coat. Technol., *168*, 2003, p. 263.
[5] APACHITEI, I.—DUSZCZYK, J.—KATGERMAN, L.—OVERKAMP, P. J. B.: Scripta Mater., *38*, 1998, p. 1347.
[6] GROSJEAN, A.—REZRAZI, M. —TAKADOUM, J.—BERCOT, P.: Surf. Coat. Technol., *137*, 2001, p. 92.
[7] BALARAJU, J. N.—KALAVATI, K.—RAJAM, K. S.: Surf. Coat. Technol., *200*, 2006, p. 3933.
[8] MADEJ, M.—OZIMINA, D.: Kovove Mater., *44*, 2006, p. 291.
[9] DELAUNOIS, F.—PETITJEAN, J. P.—LIENARD, P.—JACOB-DULIERE, M.: Surf. Coat. Technol., *124*, 2000, p. 201.
[10] NOVÁK, P.—VOJTĚCH, D.—ŠERÁK, J.: Surf. Coat. Technol., *200*, 2006, p. 5229.
[11] GALE, W. F.—TOTEMEIER, T. C.: Smithells Metals Reference Book. Amsterdam, Elsevier 2004.
[12] FAN, G. J.—CHOO, H.—LIAW, P. K.—LAVERNIA, E. J.: Mat. Sci. Eng., *A409*, 2005, p. 243.
[13] NIEH, T. G.—WANG, J. G.: Intermetallics, *13*, 2005, p. 377.
[14] PADMANABHAN, K. A.—DINDA, G. P.—HAHN, H.—GLEITER, H.: Mat. Sci. Eng., *A452–453*, 2007, p. 462.
[15] QUING, X.—XINGMING, G.: Int. J. Solids Struct., *43*, 2006, p. 7793.
[16] ZHENG, G. P.: Acta Mater., *55*, 2007, p. 149.
[17] GIGA, A.—KIMOTO, Y.—TAKIGAWA, Y.—HIGASHI, K.: Scripta Mater., *55*, 2006, p. 143.
[18] HAHN, H.—MONDAL, P.—PADMANABHAN, K. A.: Nanostructured Materials, *9*, 1997, p. 603.
[19] ZHOU, Y.—ERB, U.—AUST, K. T.—PALUMBO, G.: Scripta Mater., *48*, 2003, p. 825.
[20] PANDE, CH. S.—MASUMURA, R. A.: Mat. Sci. Eng., *A409*, 2005, p. 125.
[21] FARKAS, D.—CURTIN, W. A.: Mat. Sci. Eng., *A412*, 2005, p. 316.
[22] TAKEUCHI, S.: Scripta Mater., *44*, 2001, p. 1483.